ACS OMEGA

http://pubs.acs.org/journal/acsodf

Article

Metabolomic Elucidation of the Effect of Sucrose on the Secondary Metabolite Profiles in *Melissa officinalis* by Ultraperformance Liquid Chromatography−Mass Spectrometry

Sooah Kim, Jungyeon Kim, Nahyun Kim, Dongho Lee, Hojoung Lee, Dong-Yup Lee,* and Kyoung Heon Kim*

Cite This: *ACS Omega* 2020, 5, 33186−33195

Read Online

ACCESS | Metrics & More | Article Recommendations | Supporting Information

ABSTRACT: Sucrose induces flavonoid accumulation in plants as a defense mechanism against various stresses. However, the relationship between the biosynthesis of flavonoids as secondary metabolites and sucrose levels remains unknown. To understand the change in flavonoid biosynthesis by sucrose, we conducted secondary metabolite profiling in *Melissa officinalis* treated with different levels of sucrose using ultraperformance liquid chromatography/quadrupole time-of-flight mass spectrometry. The partial least squares-discriminant and hierarchical clustering analyses showed significant differences in secondary metabolite profiles in *M. officinalis* at 50, 150, and 300 mM sucrose levels. The levels of 3 flavonoids such as quercetin 3-*O*-*β*-D-glucosyl-(1→2)-*β*-D-glucoside, 6-methoxyaromadendrin 3-*O*-acetate, and 3-hydroxycoumarin and 19 flavonoids including 6-methoxyaromadendrin 3-*O*-acetate, aureusidin, iridin, flavonol 3-*O*-(6-*O*-malonyl-*β*-D-glucoside) quercetin 3-*O*-glucoside, and rutin increased at 150 and 300 mM sucrose, respectively, compared to 50 mM sucrose, indicating that the flavonoids were accumulated in *M. officinalis* by a higher concentration of sucrose. This is the first investigation of the change in individual flavonoids as secondary metabolites in *M. officinalis* by varying sucrose levels, and the results demonstrate that the sucrose causes the accumulation of certain flavonoids as a defense mechanism against osmotic stress.

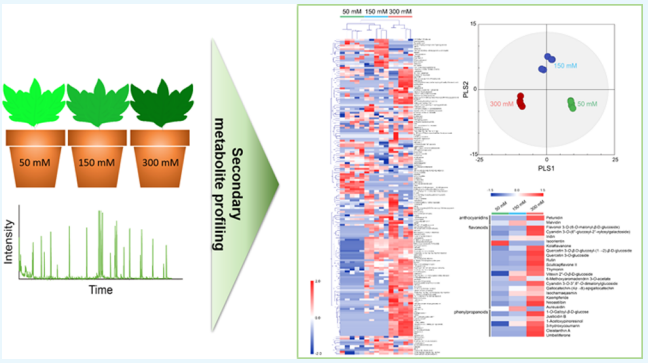

INTRODUCTION

Plants contain a variety of primary and secondary metabolites, which are the intermediate or end products of cellular processes.[1] Secondary metabolites including flavonoids play an important role in various biochemistry and physiological processes in plants. Their levels are considered important because they are used in obtaining valuable information such as the physiological state; they reflect specific biochemical processes in plants as metabolite levels serve as the ultimate response of biological systems to various genetic or environmental changes.[2]

Metabolomics, the study of chemical processes involving the entire metabolome of an organism, is a useful tool in determining metabolites in response to such changes. Various analytical tools have been used for metabolite profiling of plants, including gas chromatography/mass spectrometry,[3,4] liquid chromatography−mass spectrometry (LC−MS),[5,6] and nuclear magnetic resonance.[7,8] LC−MS is the most commonly used in secondary metabolite profiling of plants because it offers high selectivity and sensitivity and allows the analysis of nonvolatile, unstable, and high-molecular-weight compounds without derivatization.[9,10]

Melissa officinalis, a perennial herb distributed throughout East Asia, has been well known as a traditional medicine used in treating human disorders such as headache, digestion disorder, Alzheimer's disease, and cancer.[11,12] Various secondary metabolites in *M. officinalis* are known to be responsible for antioxidative, antibacterial, anti-inflammatory, antifungal, and antitumor activities.[13−16] Thus, many studies have manipulated the metabolism of *M. officinalis* to produce target secondary metabolites that can be used as valuable substances.[17,18]

Sucrose can function as the hormone-like signaling molecule and control various metabolisms and growth in plants.[19] It is an important factor affecting the synthesis of the secondary metabolites pathway including flavonoid.[20,21] Secondary metabolites are well known to accumulate during stressful

Received: October 5, 2020
Accepted: December 2, 2020
Published: December 15, 2020

Table 1. Identified Secondary Metabolites from *M. officinalis* with Retention Time and *m/z*

ESI	exact mass	mass error (ppm)	matched metabolite from database	PubChem ID
negative	242.080	19.531	lumichrome	5326566
negative	174.100	11.809	N^5-ethyl-L-glutamine	439378
negative	258.062	4.088	streptamine phosphate	439934
negative	276.025	2.137	2-carboxy-D-arabinitol 1-phosphate	129417
negative	232.016	0.655	*N*-phosphohypotaurocyamine	16019959
negative	192.063	10.309	valiolone	443630
negative	634.132	2.383	actinorhodine	441143
negative	105.033	6.208	cyanopyrazine	73172
negative	588.127	5.164	kolaflavanone	155169
negative	184.999	15.551	L-serine *O*-sulfate	164701
negative	278.115	9.500	isohelenol	15558
negative	332.074	19.246	1-*O*-galloyl-*β*-D-glucose	124021
negative	331.082	3.990	malvidin	159287
negative	504.169	7.928	cellotriose	5287993
negative	128.047	0.992	2-hydroxy-*cis*-hex-2,4-dienoate	11953951
negative	317.066	7.140	petunidin	73386
negative	110.037	8.061	catechol	289
negative	514.115	1.270	MK 571	5281888
negative	650.252	14.857	BQ 518	443291
negative	292.121	17.599	INF271	443080
negative	856.254	4.466	7-hydroxylpradimicin A	441176
negative	342.110	14.691	3-(4-methoxyphenyl)-5,6,7-trimethoxy-4*H*-1-benzopyran-4-one	248269
negative	674.221	18.819	premithramycin A2′	443797
negative	326.121	8.104	robinobiose	441428
negative	490.171	19.730	BMS-268770	56928083
negative	344.108	12.008	TRAM-34	656734
negative	328.102	16.053	7-hydroxy-6-methyl-8-ribityl lumazine	440869
negative	518.159	0.550	esmeraldic acid	443632
negative	216.027	4.060	5-carboxymethyl-2-hydroxymuconate	54675765
negative	192.047	6.535	6-(allylthio)purine	3633259
negative	133.038	11.861	L-aspartate	5960
negative	405.100	5.991	cefaloglycin	19150
negative	356.098	17.147	Bay-K-8644	2303
negative	168.019	12.028	butanoylphosphate	266
negative	307.069	14.055	narciclasine	72376
negative	150.032	1.013	*α*-oxo-benzeneacetic acid	11915
negative	471.150	4.355	10-formyldihydrofolate	135398690
negative	194.063	1.680	6-(isopropylthio)purine	3698120
negative	273.086	10.110	brugine	442998
negative	296.105	18.929	calophyllin B	5281624
negative	109.900	6.524	calcium chloride anhydrous	5284359
negative	296.092	19.494	2,3,9,10-tetrahydroxyberberine	443768
negative	332.069	10.829	hypoxylone	442747
negative	310.121	18.357	7-hydroxy-3-(4-methoxyphenyl)-4-propyl-2*H*-1-benzopyran-2-one	5357444
negative	306.060	18.751	isoprothiolane sulfoxide	93275
negative	312.106	11.416	6-*O*-(*β*-D-xylopyranosyl)-*β*-D-glucopyranose	443248
negative	814.211	3.276	victorin C	21549934
negative	506.100	7.917	cassiamin C	442728
negative	392.199	8.060	abyssinone VI	5281219
negative	610.153	1.052	rutin	5280805
negative	372.100	0.836	ohioensin-A	442531
negative	594.159	10.092	vitexin 2″-*O*-*β*-D-glucoside	5280641
negative	464.096	9.183	quercetin 3-*O*-glucoside	5280804
negative	294.021	15.387	4-[2,2-dichloro-1-(4-methoxyphenyl)ethenyl]phenol	156639
negative	448.101	7.367	isoorientin	114776
negative	360.085	15.746	thymonin	442662
negative	575.058	16.657	isopentenyladenosine-5′-triphosphate	23724748
negative	522.137	7.259	iridin	5281777
negative	342.074	17.721	dihydromethylsterigmatocystin	5280636
negative	516.127	7.769	1,3-dicaffeoylquinic acid	6474640
negative	580.312	11.523	hordatine B	72193633

https://dx.doi.org/10.1021/acsomega.0c04745
ACS Omega 2020, 5, 33186−33195

Table 1. continued

ESI	exact mass	mass error (ppm)	matched metabolite from database	PubChem ID
negative	870.218	14.415	iresinin I	11953907
negative	714.486	11.184	(2′*S*)-deoxymyxol 2′-α-L-fucoside	23724611
negative	487.120	5.943	luciferyl sulfate	11953812
negative	486.116	6.751	flavonol 3-*O*-(6-*O*-malonyl-β-D-glucoside)	11953833
negative	463.074	3.945	N^6-(1,2-dicarboxyethyl)-AMP	447145
negative	286.048	2.426	aureusidin	5281220
negative	136.039	17.392	hypoxanthine	135398638
negative	198.039	3.888	2,4-dinitrophenylhydrazine	3772977
negative	719.446	19.427	erythromycin C	83933
negative	432.194	12.242	aspulvinone H	54675755
negative	743.204	15.328	cyanidin 3-*O*-(6″-glucosyl-2″-xylosylgalactoside)	441671
negative	181.038	19.968	2-methyl-3-hydroxy-5-formylpyridine-4-carboxylate	440898
negative	374.058	7.988	glucocochlearin	5281135
negative	364.095	19.154	justicidin B	442882
negative	750.140	16.841	UDP-*N*-acetylmuramoyl-L-alanine	3037124
negative	560.081	17.449	dTDP-4-oxo-5-*C*-methyl-L-rhamnose	443215
negative	494.121	13.369	5′-methoxyhydnocarpin-D	5281879
negative	538.111	9.840	lithospermic acid	6441498
negative	493.098	18.917	MK826	443580
negative	664.382	2.599	phytolaccoside B	441939
negative	344.074	11.436	theogallin	442988
negative	374.100	17.102	scullcapflavone II	124211
negative	164.069	10.386	β-D-fucose	439650
negative	685.357	12.321	avadharidine	441710
negative	162.017	18.924	allicin	65036
negative	586.314	19.530	5-oxoavermectin “2b” aglycone	11953969
negative	584.310	13.431	lappaconitine	5281279
negative	336.059	15.581	2,2-bis(4-hydroxyphenyl)hexafluoropropane	73864
negative	652.315	11.849	thalidasine	159795
negative	608.289	19.119	oxyacanthine	442333
negative	380.216	5.889	4,4-difluoro-17-β-hydroxyandrost-5-en-3-one propionate	253787
negative	568.305	5.251	adouetine Y	5281578
negative	626.148	4.216	quercetin 3-*O*-β-D-glucosyl-(1→2)-β-D-glucoside	5282166
negative	660.424	8.099	12-*O*-palmitoyl-16-hydroxyphorbol 13-acetate	334044
negative	1051.605	14.892	aculeacin A	14315169
negative	137.905	1.711	Ba^{2+}	104810
positive	305.939	2.050	3-iodo-4-hydroxyphenylpyruvate	440184
positive	542.121	11.040	isochamaejasmin	390361
positive	184.023	3.201	5-hydroxyisourate	250388
positive	543.110	11.677	CMP-3-deoxy-D-manno-octulosonate	445888
positive	292.132	11.326	SB 206553	5163
positive	146.069	6.737	D-glutamine	145815
positive	115.063	14.931	proline	145742
positive	129.043	1.863	5-oxoproline	7405
positive	303.137	0.083	evodiamine	442088
positive	117.079	9.054	L-valine	6287
positive	324.106	4.923	D-fructofuranose 1,2′:2,3′-dianhydride	440332
positive	307.084	6.429	glutathione	124886
positive	334.057	1.241	nicotinamide D-ribonucleotide	14180
positive	450.116	4.305	neoastilbin	442437
positive	305.028	13.271	2,4-dinitro-1-(3-nitrophenoxy)benzene	221812
positive	303.007	18.316	2-(((3,5-dichlorophenyl)carbamoyl)oxy)-2-methyl-3-butenoic acid	119359
positive	900.168	18.543	*N*-methylanthraniloyl-CoA	24883420
positive	162.032	2.679	umbelliferone	5281426
positive	540.163	1.405	cleistanthin A	442833
positive	621.109	14.679	cyanidin 3-*O*-3″,6″-*O*-dimalonylglucoside	23724697
positive	360.085	3.860	6-methoxyaromadendrin 3-*O*-acetate	442415
positive	522.110	1.595	cefoselis	5748845
positive	162.032	2.617	3-hydroxycoumarin	13650
positive	610.132	0.389	gallocatechin-(4α→8)-epigallocatechin	442682
positive	341.054	18.994	aristolochic acid	2236

https://dx.doi.org/10.1021/acsomega.0c04745
ACS Omega 2020, 5, 33186−33195

Table 1. continued

ESI	exact mass	mass error (ppm)	matched metabolite from database	PubChem ID
positive	492.090	14.101	carmine	14950
positive	249.173	4.366	lophocerine	442313
positive	338.045	7.327	UK-47265	133777
positive	606.237	17.505	cancentrine	5462434
positive	418.324	9.894	8′-apo-β-carotenol	5280991
positive	436.334	8.296	2-phytyl-1,4-naphthoquinone	56927684
positive	300.063	2.857	kaempferide	5281666
positive	416.147	0.577	1-acetoxypinoresinol	442831
positive	348.169	1.303	enalaprilate	5462501
positive	892.534	2.918	zeaxanthin diglucoside	10533723
positive	183.977	11.963	3-phosphonooxypyruvate	105
positive	801.531	14.884	PC(20:4(8Z,11Z,14Z,17Z)/18:4(6Z,9Z,12Z,15Z)/0:0)	none
positive	803.547	9.142	PC(22:6(4Z,7Z,10Z,13Z,16Z,19Z)/16:1(9Z)/0:0)	none
positive	260.116	10.860	maculosin	119404
positive	884.542	8.209	PI(20:4(8Z,11Z,14Z,17Z)/18:1(11Z))	53480105
positive	743.547	10.424	PC(15:0/18:2(9Z,12Z)/0:0)	none
positive	777.531	14.567	PC(22:5(7Z,10Z,13Z,16Z,19Z)/14:1(9Z)/0:0)	none
positive	781.562	15.183	PC(20:3(5Z,8Z,11Z)/16:1(9Z)/0:0)	none
positive	755.547	15.502	PC(18:3(6Z,9Z,12Z)/16:0/0:0)	none
positive	779.547	14.305	PC(16:1(9Z)/20:4(5Z,8Z,11Z,14Z)/0:0)	none
positive	757.562	13.641	PE(15:0/22:2(13Z,16Z)/0:0)	none
positive	753.531	4.492	PC(20:3(5Z,8Z,11Z)/14:1(9Z)/0:0)	none
positive	774.528	16.736	oligomycin C	5281901
positive	596.459	0.803	spirilloxanthin	5366506
positive	612.475	17.956	DG(14:1(9Z)/22:5(4Z,7Z,10Z,13Z,16Z)/0:0)	53477996
positive	313.914	6.671	tiron	9001
positive	739.515	0.965	PE(18:2(9Z,12Z)/18:2(9Z,12Z)/0:0)	none
positive	741.531	5.923	PE(18:1(11Z)/18:2(9Z,12Z)/0:0)	none
positive	713.500	11.815	PE(20:3(5Z,8Z,11Z)/14:0/0:0)	none
positive	737.500	9.720	PE(14:1(9Z)/22:4(7Z,10Z,13Z,16Z)/0:0)	none
positive	206.006	0.849	3-oxalomalate	5459790
positive	336.140	2.553	steroid *O*-sulfate	439761
positive	715.515	5.771	PE(20:2(11Z,14Z)/14:0/0:0)	none
positive	208.001	1.808	stipitatonate	54746226
positive	636.341	18.127	ansatrienin A	5282069
positive	329.116	5.177	2,2′-(1-phenyl-1*H*-1,2,4-triazole-3,5-diyl)bisphenol	443276
positive	716.502	18.708	1′-hydroxy-γ-carotene glucoside	23724600
positive	328.116	5.397	anisatin	115121
positive	332.142	3.872	1-dehydro-9-fluoro-11-oxotestololactone	253326
positive	330.139	1.981	17α-chloroethynylestradiol	245467
positive	499.297	1.360	tauroursodeoxycholic acid	9848818
positive	155.982	15.912	2-phosphoglycolate	529
positive	477.316	0.573	gentamicin C1	72395
positive	757.599	16.260	PE(20:1(11Z)/dm18:0/0:0)	none
positive	171.952	6.659	4-bromophenol	7808
positive	168.972	12.949	2-aminoethylarsonate	129501
positive	168.964	10.786	L-selenocysteine	6326983

conditions because of defense mechanisms in plants.[22] For example, flavonoids accumulate in the presence of sucrose as defense mechanisms against osmotic stress in plants.[20,21,23] In these studies, analysis of gene expression or total flavonoid levels revealed that sucrose induces the upregulation of flavonoid biosynthesis. However, to our knowledge, there is no study on the relationship between flavonoid biosynthesis and sucrose levels through metabolite profiles, especially the individual levels of flavonoids.

In this study, the secondary metabolite profile changes in *M. officinalis* were analyzed in response to different levels of sucrose. To accomplish this, we used ultraperformance liquid chromatography-quadrupole time-of-flight mass spectrometry (UPLC-Q-TOF MS), and the metabolite profiles were statistically analyzed using partial least squares-discriminant analysis (PLS-DA) and hierarchical clustering analysis (HCA). These results can be used in understanding the alteration in metabolisms based on the sucrose level and give clues on the molecular breeding of plants for overproducing high-value metabolites.

RESULTS AND DISCUSSION

Identification of Secondary Metabolites from *M. officinalis*. To analyze the changes in the profile of secondary

https://dx.doi.org/10.1021/acsomega.0c04745
ACS Omega 2020, 5, 33186−33195

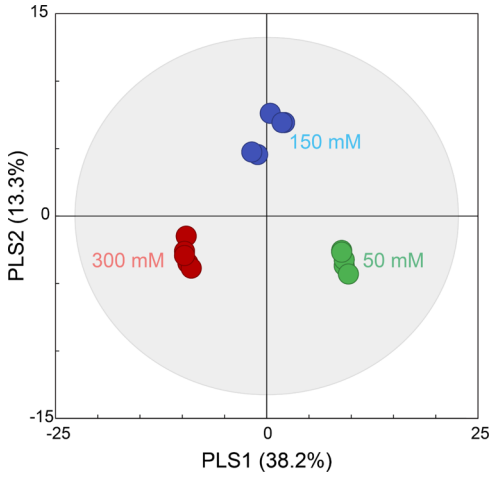

Figure 1. PLS-DA score plot of secondary metabolite profiles in *M. officinalis* treated with 50 (control; green), 150 (blue), and 300 mM (red).

metabolites of *M. officinalis* in response to sucrose, *M. officinalis* leaves treated with 50, 150, or 300 mM sucrose were extracted with MeOH and analyzed using UPLC-Q-TOF MS. More than 20,000 peaks of the negative electrospray ionization mode (ESI^-) and positive electrospray ionization ions (ESI^+) were detected, and 169 metabolites were identified using XCMS in all the 15 samples obtained from five biological replicates of each condition group (Table 1), indicating that our results were more accurate and less biased than the previous reports that showed metabolic changes under the stressful conditions with 6 unidentified secondary metabolites using LC−MS/MS,[24] 30 identified secondary metabolites using UPLC-Q-TOF MS,[25] and 95 identified metabolites using LC−MS/MS.[26] These metabolites were found to be major intermediates in the secondary metabolisms of plants, including the biosynthesis of carotenoids (e.g., (2′S)-deoxymyxol 2′-α-L-fucoside), phenylpropanoids (e.g., 1-*O*-galloyl-β-D-glucose, justicidin B, 1-acetoxypinoresinol, 3-hydroxycoumarin, cleistanthin A, and umbelliferone), flavones, and flavonols (e.g., scullcapflavone II, flavonol 3-*O*-(6-*O*-malonyl-β-D-glucoside), cyanidin 3-*O*-(6″-glucosyl-2″-xylosylgalactoside), iridin, isoorientin, kolaflavanone, thymonin, quercetin 3-*O*-glucoside, quercetin 3-*O*-β-D-glucosyl-(1→2)-β-D-glucoside, rutin, vitexin 2″-*O*-β-D-glucoside, malvidin, and petunidin).

The secondary metabolites identified in this study are well known to have beneficial health effects. For example, rutin, lithospermic acid, moxalactam, isoorientin, 5′-methoxyhydnocarpin-D, oxyacanthine, 1,3-dicaffeoylquinic acid, isohelenol, lappaconitine, phytolaccoside B, iridin, and scullcapflavone II are known to possess various physiological activities such as antioxidative,[27] antibacterial,[28] hepatoprotective,[29] anti-HIV-1,[30] antifungal,[31] antimutagenic,[32] and anti-inflammatory[33] activities. Specifically, malvidin, a primary plant pigment, inhibits human leukemia cells by arresting the G_2/M phase and then inducing apoptosis.[34] Lithospermic acid can be used in diabetic retinopathy and mesenteric ischemia reperfusion injury because of its antioxidative, hepatoprotective, and anti-inflammatory effects.[27,35]

PLS-DA of the Sucrose Effect on Secondary Metabolite Profiles. To statistically compare changes in the profile of secondary metabolites of *M. officinalis* in response to different levels of sucrose, principal component analysis (PCA) was performed using SIMCA-P+. Because the metabolite profiles of the groups were slightly discriminated by PCA, with 0.52 of R^2X and 0.33 of Q^2 (data not shown), PLS-DA was employed to obtain better separations between the groups. Among the three groups treated with sucrose levels of 50, 150, and 300 mM, the metabolite profiles were clearly separated by partial least squares 1 (PLS1) and 2 (PLS2) in the score plot of PLS-DA (Figure 1). The model generated explained variation values, such as 0.52 of R^2X and 0.97 of R^2Y, and a predictive capability value, such as 0.87 of cumulative Q^2, indicating a good model. Our previous study on the change in flavonoid levels in lemon balm by sucrose also showed that six

Table 2. Top 20 Identified Metabolites with High Absolute Loadings on PLS1 and PLS2 as Determined by PLS-DA

PLS1		PLS2	
metabolite	loading	metabolite	loading
anisatin	0.113	10-formyldihydrofolate	0.197
2,2′-(1-phenyl-1*H*-1,2,4-triazole-3,5-diyl)bisphenol	0.107	2,4-dinitrophenylhydrazine	0.159
quercetin 3-*O*-β-D-glucosyl-(1→2)-β-D-glucoside	0.107	2-carboxy-D-arabinitol 1-phosphate	0.157
isohelenol	0.101	2-methyl-3-hydroxy-5-formylpyridine-4-carboxylate	0.112
L-aspartate	0.092	5′-methoxyhydnocarpin-D	0.138
thalidasine	0.091	7-hydroxy-6-methyl-8-ribityl lumazine	0.134
aspulvinone H	0.091	allicin	0.132
2,2-bis(4-hydroxyphenyl)hexafluoropropane	0.091	α-oxo-benzeneacetic acid	0.130
allicin	0.090	Ba^{2+}	0.120
6-*O*-(β-D-xylopyranosyl)-β-D-glucopyranose	0.090	butanoylphosphate	0.115
isopentenyladenosine-5′-triphosphate	−0.115	CMP-3-deoxy-D-manno-octulosonate	−0.107
6-methoxyaromadendrin 3-*O*-acetate	−0.115	DG(14:1(9Z)/22:5(4Z,7Z,10Z,13Z,16Z)/0:0)	−0.107
BMS-268770	−0.115	5-oxoproline	−0.109
2,4-dinitrophenylhydrazine	−0.115	1-dehydro-9-fluoro-11-oxotestololactone	−0.115
gentamicin C1	−0.115	cassiamin C	−0.121
iridin	−0.118	cellotriose	−0.121
3-hydroxycoumarin	−0.118	victorin C	−0.130
cefoselis	−0.119	rutin	−0.132
lithospermic acid	−0.119	thalidasine	−0.132
dihydromethylsterigmatocystin	−0.123	quercetin 3-*O*-β-D-glucosyl-(1→2)-β-D-glucoside	−0.141

https://dx.doi.org/10.1021/acsomega.0c04745
ACS Omega 2020, 5, 33186−33195

Table 3. VIP Scores of the 78 Metabolites with a VIP >1.0 That Strongly Contributed to the PLS-DA Model

metabolite	VIP	metabolite	VIP
2-methyl-3-hydroxy-5-formylpyridine-4-carboxylate	1.772	catechol	1.190
narciclasine	1.598	scullcapflavone II	1.182
glutathione	1.588	lithospermic acid	1.173
allicin	1.500	*N*-methylanthraniloyl-CoA	1.170
α-oxo-benzeneacetic acid	1.417	iridin	1.168
quercetin 3-*O*-β-D-glucosyl-(1→2)-β-D-glucoside	1.400	gallocatechin-(4α→8)-epigallocatechin	1.168
PE(15:0/22:2(13Z,16Z)/0:0)	1.400	2-(((3,5-dichlorophenyl)carbamoyl)oxy)-2-methyl-3-butenoic acid	1.158
phytolaccoside B	1.378	PC(22:6(4Z,7Z,10Z,13Z,16Z,19Z)/16:1(9Z)/0:0)	1.156
N^6-(1,2-dicarboxyethyl)-AMP	1.377	dihydromethylsterigmatocystin	1.151
iresinin I	1.375	vitexin 2″-*O*-β-D-glucoside	1.149
rutin	1.366	evodiamine	1.143
10-formyldihydrofolate	1.363	lophocerine	1.142
umbelliferone	1.360	CMP-3-deoxy-D-manno-octulosonate	1.138
cassiamin C	1.359	aureusidin	1.116
PC(18:3(6Z,9Z,12Z)/16:0/0:0)	1.355	INF271	1.115
victorin C	1.350	BQ 518	1.113
2-carboxy-D-arabinitol 1-phosphate	1.343	tauroursodeoxycholic acid	1.110
cleistanthin A	1.338	isohelenol	1.104
2,4-dinitrophenylhydrazine	1.332	hypoxanthine	1.101
5′-methoxyhydnocarpin-D	1.330	isopentenyladenosine-5′-triphosphate	1.093
gentamicin C1	1.318	2,2′-(1-phenyl-1*H*-1,2,4-triazole-3,5-diyl)bisphenol	1.082
6-methoxyaromadendrin 3-*O*-acetate	1.317	PC(20:3(5Z,8Z,11Z)/16:1(9Z)/0:0)	1.075
flavonol 3-*O*-(6-*O*-malonyl-β-D-glucoside)	1.316	UDP-*N*-acetylmuramoyl-L-alanine	1.065
luciferyl sulfate	1.311	PE(20:3(5Z,8Z,11Z)/14:0/0:0)	1.060
erythromycin C	1.302	cellotriose	1.057
5-oxoproline	1.297	BMS-268770	1.056
1-dehydro-9-fluoro-11-oxotestololactone	1.290	3-iodo-4-hydroxyphenylpyruvate	1.056
3-hydroxycoumarin	1.279	6-(isopropylthio)purine	1.053
proline	1.274	carmine	1.053
thymonin	1.271	butanoylphosphate	1.046
L-selenocysteine	1.252	DG(14:1(9Z)/22:5(4Z,7Z,10Z,13Z,16Z)/0:0)	1.045
cefoselis	1.250	anisatin	1.043
PC(22:5(7Z,10Z,13Z,16Z,19Z)/14:1(9Z)/0:0)	1.233	4-[2,2-dichloro-1-(4-methoxyphenyl)ethenyl]phenol	1.042
thalidasine	1.226	PI(20:4(8Z,11Z,14Z,17Z)/18:1(11Z))	1.040
L-aspartate	1.214	isoorientin	1.034
7-hydroxy-6-methyl-8-ribityl lumazine	1.211	quercetin 3-*O*-glucoside	1.017
aspulvinone H	1.198	cefaloglycin	1.015
2,2-bis(4-hydroxyphenyl)hexafluoropropane	1.197	avadharidine	1.013
Ba^{2+}	1.192	justicidin B	1.009

metabolite profiles were significantly different between 50, 150, and 300 mM sucrose.[24] However, the present results may be considered more accurate and reliable because only six secondary metabolites (i.e., 435.13, 523.129, 540.063, 573.200, 615.714, and 617.153) were used in the previous study without identification. In the permutation test, all points of permuted R^2 and Q^2 values to the left were located in the lower side contrary to the original points, and the regression line of Q^2 had a negative intercept, indicating that the PLS-DA models were clearly validated without overfitting from the original model (Figure S2).[36]

The loading scores of the selected 20 metabolites, which represented the magnitude of the contribution of each metabolite to PLS, are listed in Table 2. Of the identified 169 metabolites in this study, 40 metabolites including anisatin, quercetin 3-*O*-β-D-glucosyl-(1→2)-β-D-glucoside, isohelenol, and L-aspartate contributed positively to PLS1. However, 129 metabolites such as lithospermic acid, iridin, 3-hydroxycoumarin, and 6-methoxyaromadendrin 3-*O*-acetate contributed negatively to PLS1. Seventy-nine metabolites including 10-formyldihydrofolate, 2,4-dinitrophenylhydrazine, and allicin contributed positively to PLS2, while 90 metabolites such as quercetin 3-*O*-β-D-glucosyl-(1→2)-β-D-glucoside, rutin, thalidasine, and victorin C contributed negatively to PLS2.

In variable importance in projection (VIP) analysis, VIP values greater than 1 are considered important.[36] In this study, 78 metabolites such as quercetin 3-*O*-β-D-glucosyl-(1→2)-β-D-glucoside, rutin, umbelliferone, and cleistanthin A were shown to have VIP values greater than 1, of which 16 metabolites belong to flavonoid classes (Table 3). These results suggested that the flavonoids were critical metabolites for discriminating between the groups.

HCA of the Sucrose Effect on Secondary Metabolite Profiles. To cluster and visualize the discrimination of secondary metabolite profiles with 50, 150, and 300 mM sucrose, HCA with the Euclidean distance coefficient and average linkage was performed using MeV software. After normalization using the sum of identified metabolites and then transformation using unit variance scaling, data composed of

https://dx.doi.org/10.1021/acsomega.0c04745
ACS Omega 2020, 5, 33186−33195

Figure 2. Clustered heat map of 169 secondary metabolites of *M. officinalis* treated with 50 (control; green), 150 (blue), and 300 mM (red) sucrose. Similarity assessment of clustering based on the Euclidean distance coefficient and average linkage method. Each column and each row represent different concentrations of sucrose and individual metabolite, respectively.

identified metabolites and groups (50, 150, and 300 mM sucrose) were exported into the heat map.

In the heat map, five biological replicates at each group had similar metabolite profiles (Figure 2). However, the metabolite profiles were significantly different depending on different sucrose levels, 50, 150, and 300 mM. The secondary metabolite profile of 150 mM sucrose was closer to that of 300 mM sucrose than to that of 50 mM sucrose. These results are similar to those obtained in a previous study on primary metabolite profiles in *M. officinalis* with 64 metabolites.[4] This comparison indicates that the effect of sucrose level on primary metabolite profiles may be associated with the secondary metabolite profiles in *M. officinalis*. Moreover, the clustering of secondary metabolite profiles between sucrose levels was enabled by certain individual metabolites. For example, L-serine *O*-sulfate, thalidasin, spirilloxanthin, and quercetin 3-*O*-*β*-D-glucosyl-(1→2)-*β*-D-glucoside increased in 50 mM. However, the levels of proline, glutathione, isoorientin scullcapflavone II, flavonol 3-*O*-(6-*O*-malonyl-*β*-D-glucoside), luciferyl sulfate, cassiamin C, and rutin were much higher in 300 mM sucrose than in 50 and 150 mM sucrose.

Comparison of Individual Flavonoid Levels with 50, 150, and 300 mM Sucrose. Most studies have reported only total flavonoid abundances to reveal the relationship between sucrose levels and contents of total flavonoids[20,24,37,38] or the phenylpropanoid pathway[39,40] without identifying or comparing individual flavonoid abundances. In this study, we identified individual secondary metabolites and determined the changes in each flavonoid, anthocyanindin, and phenylpropanoid levels depending on sucrose levels.

To compare the changes in flavonoid level between the groups, one-way analysis of variance with the post hoc Tukey's honestly significant difference test was conducted using Statistica ($p > 0.05$). The abundance of three flavonoids such as quercetin 3-*O*-*β*-D-glucosyl-(1→2)-*β*-D-glucoside, 6-methoxyaromadendrin 3-*O*-acetate, and 3-hydroxycoumarin increased with 150 mM sucrose compared to those with 50 mM sucrose. However, compared to those with 50 mM sucrose, the abundances of most flavonoids such as 6-methoxyaromadendrin 3-*O*-acetate, 3-hydroxycoumarin, aureusidin, thymonin, rutin, justicidin B, isoorientin, quercetin 3-*O*-glucoside, umbelliferone, iridin, scullcapflavone II, cleistanthin A, flavonol 3-*O*-(6-*O*-malonyl-*β*-glucoside), isochamaejasmin, gallocatechin-(*α*→8)-epigallocatechin, vitexin 2″-*O*-*β*-glucoside, kolaflavanone, kaempferide, and neoastilbin were significantly increased with 300 mM (Figure 3). These results showed that flavonoids accumulated depending on the sucrose level, indicating that sucrose induced the production of more flavonoids via the phenylpropanoid pathway.

Similar to these results, previous studies have reported that rutin accumulates in *Fagopyrum esculentum* Moench in response to sucrose[41] and quercetin 3-*O*-glucoside accumulates in *Arabidopsis* under abiotic and oxidative stress.[42] Our results showed that the types of accumulating flavonoids in *M. officinalis* differed depending on sucrose levels, and active flavonoid biosynthesis served as a defense mechanism against osmotic stress, suggesting that the biosynthetic pathway of flavonoids was regulated by the sucrose signaling pathway. Previously, it was observed at the messenger RNA level that sucrose caused the accumulation of anthocyanins and the upregulation of anthocyanin synthesis.[20] However, our results showed that anthocyanins (e.g., malvidin and petunidin) did not accumulate under a high sucrose level at both 150 and 300 mM. This is possibly because anthocyanins other than malvidin and petunidin were not identified in this study, and malvidin and petunidin could not represent the behaviors of all other anthocyanins under a high sucrose level. The precise prediction and speculation of the secondary metabolism and

https://dx.doi.org/10.1021/acsomega.0c04745
ACS Omega 2020, 5, 33186−33195

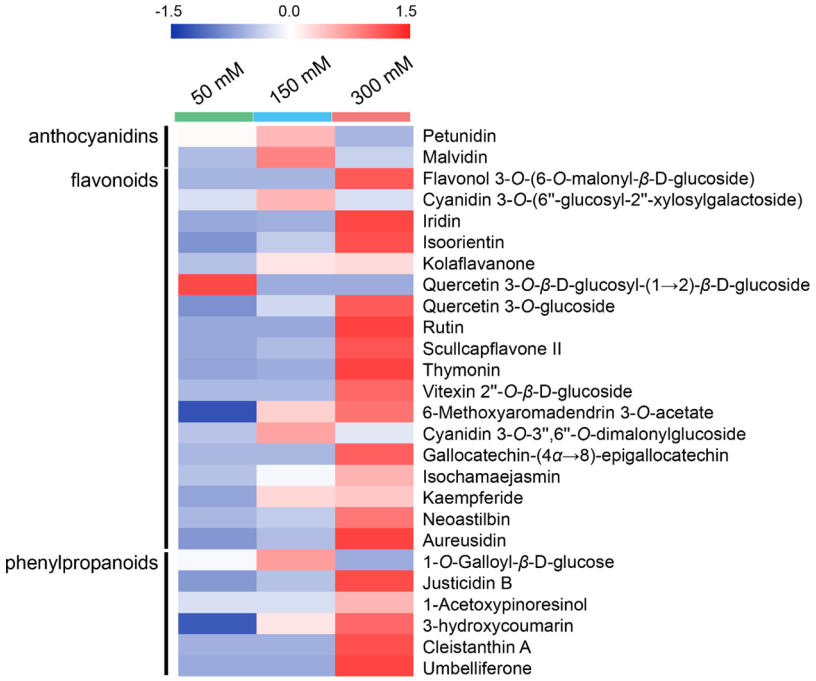

Figure 3. Heat map of 26 flavonoids in *M. officinalis* treated with 50 (control; green), 150 (blue), and 300 mM (red). Each row represents individual flavonoids.

change in individual secondary metabolites of *M. officinalis* in response to the concentrations of sucrose should be supported and verified by further experiments.

CONCLUSIONS

This is the first report to investigate the change in secondary metabolite profiles in *M. officinalis* depending on the sucrose level using UPLC-Q-TOF MS. One hundred and sixty-nine metabolites were identified using XCMS; these metabolites were major intermediates in the secondary metabolism of plants such as the biosynthesis of carotenoids, phenylpropanoids, flavones, and flavonols, which serves as a defense mechanism against stress in plants. PLS-DA and HCA results showed a significant difference in secondary metabolite profiles in *M. officinalis* between 50, 150, and 300 mM sucrose. In contrast to that with 50 mM sucrose, 32 secondary metabolites such as 6-methoxyaromadendrin 3-*O*-acetate and 3-hydroxycoumarin accumulated in 150 mM, and 76 metabolites such as aureusidin, thymonin, quercetin 3-*O*-glucoside, and rutin increased in 300 mM. Accumulation of different types of flavonoids was observed depending on the sucrose level, suggesting that the accumulation of these flavonoids acts as a defense mechanism against osmotic stress. This study demonstrated that secondary metabolite profiles could be a useful tool for investigating the change in certain secondary metabolites and secondary metabolism in plants under osmotic stress and provide clues for manipulating plant metabolisms to produce target flavonoids, which have various properties such as antitumoral, antioxidant, antifungal, and antibacterial activities.

MATERIALS AND METHODS

Plant Growth Conditions. *M. officinalis* was prepared as previously described.[4] Briefly, *M. officinalis* was cultivated in 4 g/L Murashige and Skoog medium (0.025 mg/L of $CoCl_2 \cdot 6H_2O$, 0.025 mg/L of $CuSO_4 \cdot 5H_2O$, 36.70 mg/L of FeNaEDTA, 6.20 mg/L of H_3BO_3, 0.83 mg/L of KI, 16.9 mg/L of $MnSO_4 \cdot H_2O$, 0.25 mg/L of $Na_2MoO_4 \cdot 2H_2O$, 8.60 mg/L of $ZnSO_4 \cdot 7H_2O$, 332.02 mg/L of $CaCl_2$, 170.00 mg/L of KH_2PO_4, 1900.00 mg/L of KNO_3, 180.54 mg/L of $MgSO_4$, and 1650.00 mg/L of NH_4NO_3) containing 50 mM sucrose and 7 g/L agar at pH 5.7 after 2 cm-long explants with two leaves were transferred to the culture and test media with three different concentrations of sucrose, 50 (control), 150, or 300 mM, for examining the effects of sucrose concentration on flavonoid accumulation in *M. officinalis*.[4,24] The leaves were incubated at 25 °C for 20 days (15:9 h light−dark cycle). The leaves of *M. officinalis* were harvested and quickly frozen in liquid nitrogen to quench cellular metabolism, and the frozen samples were stored at −80 °C.

Metabolite Extraction and UPLC-Q-TOF MS Analysis. Fifty milligrams of ground *M. officinalis* leaves were extracted with 0.5 mL of cold methanol (high-performance liquid chromatography grade, Merck, Darmstadt, Germany). The methanol extract was diluted with 50 μL and was thoroughly vortexed, after which it was centrifuged at 14,000*g* for 5 min. The supernatant was filtered using a 0.45 μm syringe filter (hydrophilic poly(tetrafluoroethylene), Advantec, Dublin, OH). The metabolite extract was stored at −20 °C before UPLC-Q-TOF MS analysis.

Metabolite extract was analyzed by UPLC-Q-TOF MS. The UPLC analysis was performed using a Waters ACQUITY UPLC system (Waters, Milford, MA) equipped with a Waters ACQUITY BEH C18 column (100 × 2.1 mm, 1.7 μm). The mobile phase consisted of solvent A, 0.1% (w/v) formic acid in distilled water, and solvent B, 0.1% (w/v) formic acid in acetonitrile. The UPLC was eluted first with a linear gradient from 10 to 100% of solvent B (0−7.0 min) and then eluted isocratically with 100% of solvent B (7.0−8.0 min). The flow rate was 0.3 mL/min, and the injection volume was 5 μL. The column and autosampler were maintained at 35 and 15 °C, respectively. Mass spectrometry was performed using a Q-TOF

https://dx.doi.org/10.1021/acsomega.0c04745
ACS Omega 2020, 5, 33186−33195

micromass detector (Waters, Manchester, UK). The conditions of the Q-TOF mass spectrometer in the negative electrospray ionization (ESI) mode were 2800 V of capillary voltage, 35 V of sample cone voltage, 1.0 V of extraction cone voltage, 250 °C of desolvation temperature, 100 °C of source temperature, and 500 L/h of desolvation gas flow rate. The positive ESI was under the same conditions, expect for an extraction cone voltage of 2.0 V. The ESI mass spectra were acquired over m/z 100−1500. Leucine-enkephalin was used as a reference ion by the LockSpray interface to measure mass more accurately and reproducibly.

Data Processing and Statistical Analysis. Acquired data were analyzed using Waters MassLynx (version 4.1). The noise elimination level was set at 6.0 with 10 masses per retention time being collected. Before further processing, lock spray scans were removed because lock spray peaks disrupted the detection and analysis of actual signals from samples (Figure S1A,B). UPLC-Q-TOF MS data were preprocessed using XCMS with signal-to-noise ratios as described in the literature (Table S1).[43,44] Mass and retention time windows were set at 0.05 Da and 0.20 min, respectively. After normalization by log transformation, the processed data were further analyzed using PLS-DA and HCA with the Euclidean distance coefficient and average linkage methods. SIMCA-P+ (version 14.1, Umetrics AB, Umea, Sweden) was used for PLS-DA,[36] and MeV (MultiExperiment Viewer; Dana-Farber Cancer Institute, Boston, MA) was used for HCA.[45] Statistica (version 7.1; StatSoft, Tulsa, OK) was used for the univariate analysis.[46]

■ ASSOCIATED CONTENT

Supporting Information

The Supporting Information is available free of charge at https://pubs.acs.org/doi/10.1021/acsomega.0c04745.

Chromatograms for the same samples before and after removal of lock spray scans as examples; validation of the PLS-DA model using the 100 permutation test; and number of peaks detected, peak groups, IP clusters, and predictions in negative and positive modes (PDF)

■ AUTHOR INFORMATION

Corresponding Authors

Dong-Yup Lee − *School of Chemical Engineering, Sungkyunkwan University, Suwon 25308, South Korea*; Email: dongyuplee@skku.edu

Kyoung Heon Kim − *Department of Biotechnology, Graduate School, Korea University, Seoul 02841, South Korea*; orcid.org/0000-0003-4600-8668; Phone: +82-2-3290-3028; Email: khekim@korea.ac.kr

Authors

Sooah Kim − *Department of Environment Science and Biotechnology, Jeonju University, Jeonju 55069, South Korea*

Jungyeon Kim − *Department of Biotechnology, Graduate School, Korea University, Seoul 02841, South Korea*

Nahyun Kim − *College of Life Sciences and Biotechnology, Korea University, Seoul 02841, South Korea*

Dongho Lee − *College of Life Sciences and Biotechnology, Korea University, Seoul 02841, South Korea*; orcid.org/0000-0003-4379-814X

Hojoung Lee − *College of Life Sciences and Biotechnology, Korea University, Seoul 02841, South Korea*; orcid.org/0000-0002-5626-5695

Complete contact information is available at: https://pubs.acs.org/10.1021/acsomega.0c04745

Author Contributions

K.H.K. and D.L. conceived and designed the project. S.K. and H.L. collected the samples. S.K., J.K., and N.K. performed the experiments. S.K., J.K., N.K., D.-Y.L., and D.L. acquired the metabolomics data. S.K., D.L., H.L., D.-Y.L., and K.H.K. analyzed the data. S.K., D.-Y.L., and K.H.K. wrote the manuscript.

Notes

The authors declare no competing financial interest.

■ ACKNOWLEDGMENTS

This work was supported by the Mid-career Researcher Program and Young Researcher Program from the National Research Foundation of Korea (NRF-2020R1A2B5B02002631 and NRF-2020R1G1A100826811, respectively). S.K. acknowledges the support of the Research Grant of Jeonju University in 2019. Facility support at the Korea University Food Safety Hall by the Institute of Biomedical Science and Food Safety is also acknowledged.

■ REFERENCES

(1) Fiehn, O. Metabolomics—the link between genotypes and phenotypes. *Plant Mol. Biol.* **2002**, *48*, 155−171.

(2) Weckwerth, W. Metabolomics in systems biology. *Annu. Rev. Plant Biol.* **2003**, *54*, 669−689.

(3) Fiehn, O.; Kopka, J.; Trethewey, R. N.; Willmitzer, L. Identification of uncommon plant metabolites based on calculation of elemental compositions using gas chromatography and quadrupole mass spectrometry. *Anal. Chem.* **2000**, *72*, 3573−3580.

(4) Kim, S.; Shin, M. H.; Hossain, M. A.; Yun, E. J.; Lee, H.; Kim, K. H. Metabolite profiling of sucrose effect on the metabolism of *Melissa officinalis* by gas chromatography-mass spectrometry. *Anal. Bioanal. Chem.* **2011**, *399*, 3519−3528.

(5) Theodoridis, G.; Gika, H.; Franceschi, P.; Caputi, L.; Arapitsas, P.; Scholz, M.; Masuero, D.; Wehrens, R.; Vrhovsek, U.; Mattivi, F. LC-MS based global metabolite profiling of grapes: solvent extraction protocol optimisation. *Metabolomics* **2012**, *8*, 175−185.

(6) Matsuda, F.; Yonekura-Sakakibara, K.; Niida, R.; Kuromori, T.; Shinozaki, K.; Saito, K. MS/MS spectral tag-based annotation of non-targeted profile of plant secondary metabolites. *Plant J.* **2009**, *57*, 555−577.

(7) Krishnan, P.; Kruger, N. J.; Ratcliffe, R. G. Metabolite fingerprinting and profiling in plants using NMR. *J. Exp. Bot.* **2005**, *56*, 255−265.

(8) Bundy, J. G.; Spurgeon, D. J.; Svendsen, C.; Hankard, P. K.; Osborn, D.; Lindon, J. C.; Nicholson, J. K. Earthworm species of the genus Eisenia can be phenotypically differentiated by metabolic profiling. *FEBS Lett.* **2002**, *521*, 115−120.

(9) Fraser, P. D.; Pinto, M. E. S.; Holloway, D. E.; Bramley, P. M. Application of high-performance liquid chromatography with photodiode array detection to the metabolic profiling of plant isoprenoids. *Plant J.* **2000**, *24*, 551−558.

(10) Sumner, L. W.; Mendes, P.; Dixon, R. A. Plant metabolomics: large-scale phytochemistry in the functional genomics era. *Phytochemistry* **2003**, *62*, 817−836.

(11) Tagashira, M.; Ohtake, Y. A new antioxidative 1,3-benzodioxole from *Melissa officinalis*. *Planta Med.* **1998**, *64*, 555−558.

(12) de Sousa, A. C.; Gattass, C. R.; Alviano, D. S.; Alviano, C. S.; Blank, A. F.; Alves, P. B. *Melissa officinalis* L. essential oil: antitumoral and antioxidant activities. *J. Pharm. Pharmacol.* **2004**, *56*, 677−681.

(13) Kim, S.; Yun, E. J.; Bak, J. S.; Lee, H.; Lee, S. J.; Kim, C. T.; Lee, J.-H.; Kim, K. H. Response surface optimised extraction and

chromatographic purification of rosmarinic acid from *Melissa officinalis* leaves. *Food Chem.* **2010**, *121*, 521−526.
(14) Nikitina, V. S.; Kuz'mina, L. Y.; Melent'ev, A. I.; Shendel', G. V. Antibacterial activity of polyphenolic compounds isolated from plants of geraniaceae and rosaceae families. *Appl. Biochem. Microbiol.* **2007**, *43*, 629−634.
(15) Viollon, C.; Chaumont, J.-P. Antifungal properties of essential oils and their main components upon *Cryptococcus neoformans*. *Mycopathologia* **1994**, *128*, 151−153.
(16) Miron, T. L.; Herrero, M.; Ibáñez, E. Enrichment of antioxidant compounds from lemon balm (*Melissa officinalis*) by pressurized liquid extraction and enzyme-assisted extraction. *J. Chromatogr. A* **2013**, *1288*, 1−9.
(17) Weitzel, C.; Petersen, M. Enzymes of phenylpropanoid metabolism in the important medicinal plant *Melissa officinalis* L. *Planta* **2010**, *232*, 731−742.
(18) Kong, J.-Q. Phenylalanine ammonia-lyase, a key component used for phenylpropanoids production by metabolic engineering. *RSC Adv.* **2015**, *5*, 62587−62603.
(19) Smeekens, S.; Hellmann, H. A. Sugar sensing and signaling in plants. *Front. Plant Sci.* **2014**, *5*, 113.
(20) Solfanelli, C.; Poggi, A.; Loreti, E.; Alpi, A.; Perata, P. Sucrose-specific induction of the anthocyanin biosynthetic pathway in Arabidopsis. *Plant Physiol.* **2006**, *140*, 637−646.
(21) Zheng, Y.; Tian, L.; Liu, H.; Pan, Q.; Zhan, J.; Huang, W. Sugars induce anthocyanin accumulation and flavanone 3-hydroxylase expression in grape berries. *Plant Growth Regul.* **2009**, *58*, 251−260.
(22) Bennett, R. N.; Wallsgrove, R. M. Secondary metabolites in plant defence mechanisms. *New Phytol.* **1994**, *127*, 617−633.
(23) Lloyd, J. C.; Zakhleniuk, O. V. Responses of primary and secondary metabolism to sugar accumulation revealed by microarray expression analysis of the *Arabidopsis* mutant, pho3. *J. Exp. Bot.* **2004**, *55*, 1221−1230.
(24) Hossain, M. A.; Kim, S.; Kim, K. H.; Lee, S.-J.; Lee, H. Flavonoid compounds are enriched in lemon balm (*Melissa officinalis*) leaves by a high level of sucrose and confer increased antioxidant activity. *Hortscience* **2009**, *44*, 1907−1913.
(25) Pant, B.-D.; Pant, P.; Erban, A.; Huhman, D.; Kopka, J.; Scheible, W.-R. Identification of primary and secondary metabolites with phosphorus status-dependent abundance in Arabidopsis, and of the transcription factor PHR1 as a major regulator of metabolic changes during phosphorus limitation. *Plant, Cell Environ.* **2015**, *38*, 172−187.
(26) Matsuda, F.; Yonekura-Sakakibara, K.; Niida, R.; Kuromori, T.; Shinozaki, K.; Saito, K. MS/MS spectral tag-based annotation of non-targeted profile of plant secondary metabolites. *Plant J.* **2009**, *57*, 555−577.
(27) Jin, C. J.; Yu, S. H.; Wang, X.-M.; Woo, S. J.; Park, H. J.; Lee, H. C.; Choi, S. H.; Kim, K. M.; Kim, J. H.; Park, K. S.; Jang, H. C.; Lim, S. The effect of lithospermic acid, an antioxidant, on development of diabetic retinopathy in spontaneously obese diabetic rats. *PLoS One* **2014**, *9*, No. e98232.
(28) Huang, C.; Zheng, B. W.; Yu, W.; Niu, T. S.; Xiao, T. T.; Zhang, J.; Xiao, Y. H. Antibacterial effect evaluation of moxalactam against extended-spectrum beta-lactamase-producing *Escherichia coli* and *Klebsiella pneumoniae* with in vitro pharmacokinetics/pharmaco-dynamics simulation. *Infect. Drug Resist.* **2018**, *11*, 103−112.
(29) Huang, Q. F.; Zhang, S. J.; Zheng, L.; Liao, M.; He, M.; Huang, R. B.; Zhuo, L.; Lin, X. Protective effect of isoorientin-2 ″-O-alpha-L-arabinopyranosyl isolated from *Gypsophila elegans* on alcohol induced hepatic fibrosis in rats. *Food Chem. Toxicol.* **2012**, *50*, 1992−2001.
(30) Varadaraju, T. G.; Hwu, J. R. Synthesis of anti-HIV lithospermic acid by two diverse strategies. *Org. Biomol. Chem.* **2012**, *10*, 5456−5465.
(31) Escalante, A.; Gattuso, M.; Pérez, P.; Zacchino, S. Evidence for the mechanism of action of the antifungal phytolaccoside B isolated from phytolacca tetramera hauman. *J. Nat. Prod.* **2008**, *71*, 1720−1725.
(32) Wozniak, D.; Janda, B.; Kapusta, I.; Oleszek, W.; Matkowski, A. Antimutagenic and anti-oxidant activities of isoflavonoids from *Belamcanda chinensis* (L.) DC. *Mutat. Res., Genet. Toxicol. Environ. Mutagen.* **2010**, *696*, 148−153.
(33) Jang, H.-Y.; Ahn, K.-S.; Park, M.-J.; Kwon, O.-K.; Lee, H.-K.; Oh, S.-R. Skullcapflavone II inhibits ovalbumin-induced airway inflammation in a mouse model of asthma. *Int. Immunopharmacol.* **2012**, *12*, 666−674.
(34) Hyun, J. W.; Chung, H. S. Cyanidin and malvidin from Oryza sativa cv. Heugjinjubyeo mediate cytotoxicity against human monocytic leukemia cells by arrest of G(2)/M phase and induction of apoptosis. *J. Agric. Food Chem.* **2004**, *52*, 2213−2217.
(35) Chan, K. W. K.; Ho, W. S. Anti-oxidative and hepatoprotective effects of lithospermic acid against carbon tetrachloride-induced liver oxidative damage *in vitro* and *in vivo*. *Oncol. Rep.* **2015**, *34*, 673−680.
(36) Umetrics, A. B. *User's Guide to SIMCA-P, SIMCA-P+ version 11.0*; Umetrics AB: UmeÅ, Sweden, 2005.
(37) Gollop, R.; Even, S.; Colova-Tsolova, V.; Perl, A. Expression of the grape dihydroflavonol reductase gene and analysis of its promoter region. *J. Exp. Bot.* **2002**, *53*, 1397−1409.
(38) Pasqua, G.; Monacelli, B.; Mulinacci, N.; Rinaldi, S.; Giaccherini, C.; Innocenti, M.; Vinceri, F. F. The effect of growth regulators and sucrose on anthocyanin production in Camptotheca acuminata cell cultures. *Plant Physiol. Biochem.* **2005**, *43*, 293−298.
(39) Li, Y.; Van den Ende, W.; Rolland, F. Sucrose induction of anthocyanin biosynthesis Is bediated by DELLA. *Mol. Plant* **2014**, *7*, 570−572.
(40) Payyavula, R. S.; Singh, R. K.; Navarre, D. A. Transcription factors, sucrose, and sucrose metabolic genes interact to regulate potato phenylpropanoid metabolism. *J. Exp. Bot.* **2013**, *64*, 5115−5131.
(41) Li, X.; Park, N. I.; Park, C. H.; Kim, S. G.; Lee, S. Y.; Park, S. U. Influence of sucrose on rutin content and flavonoid biosynthetic gene expression in seedlings of common buckwheat (Fagopyrum esculentum Moench). *Plant Omics* **2011**, *4*, 215−219.
(42) Nakabayashi, R.; Yonekura-Sakakibara, K.; Urano, K.; Suzuki, M.; Yamada, Y.; Nishizawa, T.; Matsuda, F.; Kojima, M.; Sakakibara, H.; Shinozaki, K.; Michael, A. J.; Tohge, T.; Yamazaki, M.; Saito, K. Enhancement of oxidative and drought tolerance in Arabidopsis by overaccumulation of antioxidant flavonoids. *Plant J.* **2014**, *77*, 367−379.
(43) Lee, T. S.; Ho, Y. S.; Yeo, H. C.; Lin, J. P. Y.; Lee, D.-Y. Precursor mass prediction by clustering ionization products in LC-MS-based metabolomics. *Metabolomics* **2013**, *9*, 1301−1310.
(44) Huan, T.; Forsberg, E. M.; Rinehart, D.; Johnson, C. H.; Ivanisevic, J.; Benton, H. P.; Fang, M.; Aisporna, A.; Hilmers, B.; Poole, F. L.; Thorgersen, M. P.; Adams, M. W. W.; Krantz, G.; Fields, M. W.; Robbins, P. D.; Niedernhofer, L. J.; Ideker, T.; Majumder, E. L.; Wall, J. D.; Rattray, N. J. W.; Goodacre, R.; Lairson, L. L.; Siuzdak, G. Systems biology guided by XCMS Online metabolomics. *Nat. Methods* **2017**, *14*, 461−462.
(45) Saeed, A. I.; Bhagabati, N. K.; Braisted, J. C.; Liang, W.; Sharov, V.; Howe, E. A.; Li, J.; Thiagarajan, M.; White, J. A.; Quackenbush, J. TM4 microarray software suite. *Methods Enzymol.* **2006**, *411*, 134−193.
(46) Lee, D. Y.; Fiehn, O. High quality metabolomic data for *Chlamydomonas reinhardtii*. *Plant Methods* **2008**, *4*, 7.

https://dx.doi.org/10.1021/acsomega.0c04745
ACS Omega 2020, 5, 33186−33195